

Josephson current and density of states in proximity circuits with s^{+-} superconductors

Stanislav Apostolov and Alex Levchenko

Department of Physics and Astronomy, Michigan State University, East Lansing, Michigan 48824, USA

(Dated: December 1, 2012)

We study the emergent proximity effect in mesoscopic circuits that involve a conventional superconductor and an unconventional pnictide superconductor separated by a diffusive normal or ferromagnetic wire. The focus is placed on revealing signatures of the proposed s^{+-} state of pnictides from the proximity-induced density of states and Josephson current. We find analytically a universal result for the density of states that exhibits both the Thouless gap at low energies, and peculiar features near the superconducting gap edges at higher energies. The latter may be used to discriminate between s^{+-} and s^{++} symmetry scenarios in scanning tunneling spectroscopy experiments. We also calculate Josephson current-phase relationships for different junction configurations, which are found to display robust $0-\pi$ transitions for a wide range of parameters.

PACS numbers: 74.45.+c, 74.50.+r, 74.70.Xa, 74.78.Na

I. INTRODUCTION

The origin of unconventional superconductivity in ferropnictide compounds, their phase diagram and symmetry of the underlying order parameter are topics that attract considerable interest in recent years, see Refs. 1–3 for reviews. Superconductivity in pnictides emerges in close proximity to an antiferromagnetically ordered state, and the critical temperature T_c has a dome-shaped dependence on doping^{4,5} similar to that in cuprates. Due to their multiband electronic structure with multiple Fermi surfaces and delicate interplay of interactions in different channels a number of possibilities for electron ordering are possible.^{6–8} Structural transition, competing or co-existing magnetic spin-density-wave (SDW) and superconducting (SC) orders are being examples. The latter may be in the form of the conventional s^{++} -wave state that has s -wave symmetry in the Brillouin zone and gaps of the same sign on electron and holes Fermi surfaces. Alternatively, SC order may appear in the form of an extended s^{+-} state that looks as s -wave from a symmetry point of view but has opposite signs of the gaps on different sheets of the Fermi surfaces.^{9–11} There may be scenarios of several SC states with the nodes in the SC gap, of both s -wave and d -wave symmetries.^{12–14}

Experimentally, the most convincing support in favor of unconventional symmetry of pnictides is given so far by the observed spin resonance below T_c in inelastic neutron scattering measurements on K-doped BaFeAs.¹⁵ In all the materials studied, the resonance occurs at the antiferromagnetic wave vector Q of the parent compound. It is thought to be a triplet excitation of the singlet Cooper pairs, implying a superconducting order parameter that satisfies $\Delta(k+Q) = -\Delta(k)$, which indicates either s^{+-} or d -wave cases. Fabricated c -axis Josephson junctions of this material and ordinary superconductor are suggestive of an s -wave state, but not providing unambiguous evidence for the s^{+-} state itself.¹⁶ In addition, ab -corner-junction experiments with Co-doped BaFeAs seems to eliminate the option of d -wave pairing.¹⁷ Other notable experiments providing substantial but still indi-

rect support of s^{+-} state include quasiparticle interference in magnetic field probed by scanning tunneling microscopy¹⁸ and observation of half-integer flux-quantum jumps through the loop formed by niobium and polycrystalline iron-pnictide sample.¹⁹ Finally, there is a growing number of low-temperatures studies addressing thermodynamics and transport properties of pnictides, however it is usually hard to deduce underlying symmetry of a superconductor from such data. For fully gapped s -wave state, one expects to see exponentially suppressed quasiparticle response and power-law in temperature for the d -wave state with the nodes. The possible ambiguity in interpretation of data stems from the fact that accidental nodes on the Fermi surface or impurity-induced subgap states may easily alter low-temperature behavior of, for example, heat capacity or London penetration depth.

It is widely agreed that a decisive experiment should involve a phase sensitive probe such as the Josephson effect. Although original proposals^{20,21} followed mostly immediately after the s^{+-} candidate symmetry was introduced, no such direct measurements of the current-phase relationship have been performed so far for pnictide-based Josephson junctions. Nevertheless, this inspired a lot of theoretical efforts in finding simpler geometries or alternative signatures of s^{+-} pairing state in proximity circuits with pnictides and conventional superconductors.^{22–31} A particularly interesting recent conclusion^{24,29} is that tunneling spectra of weakly coupled s - s^{+-} bi-layers exhibit distinct features characteristic only to sign-changing symmetry of the gap. Physically, the effect comes from the frustration in the junction since the gap of an ordinary superconductor tends to align with one of the gaps of s^{+-} superconductor, and thus becomes in the conflict with the other band experiencing the anti-proximity effect.

II. THEORETICAL FRAMEWORK

In this work, we consider plethora of effects in superconductor-metal-superconductor junctions where

one or both superconductors are assumed to have s^{+-} symmetry. The metal is either normal or ferromagnetic diffusive wire. In the context of the Josephson effect, in such structures, we find various current-phase relationships whose shapes depend on the relation between the wire length and superconducting coherence length, and boundary transparency. The generic feature is non-analytical behavior of the current near phase π , which corresponds to the closing of the proximity-induced gap in the wire, and robust $0-\pi$ oscillations even without ferromagnets. In the context of the proximity-induced density of states (DOS) in the wire, we identify fingerprints of the s^{+-} symmetry, which is thus not only unique to frustrated s - s^{+-} bi-layers.

We build our calculations based on the Usadel equations³² and accompanying Kupriyanov-Lukichev boundary conditions³³ modified for a multiband case.³⁴ This quasiclassical theory captures all the essential features and full complexity of the proximity effect. Adopting angular parametrization for the normal and anomalous quasiclassical Green's functions³⁵ as $G = \cos \theta(\omega, x)$ and $F = \sin \theta(\omega, x)e^{i\chi(\omega, x)}$, Usadel equations take the form

$$\partial_x^2 \theta - (2\omega/\varepsilon_{Th}) \sin \theta = (\partial_x \chi)^2 \sin \theta \cos \theta, \quad (1a)$$

$$\partial_x (\sin^2 \theta \partial_x \chi) = 0, \quad (1b)$$

where $\omega = (2n+1)\pi T$ is Matsubara frequency, $\varepsilon_{Th} = D/L^2$ is the Thouless energy for the wire of length L , and D is the diffusion coefficient. Spatial derivatives are taken with respect to the dimensionless coordinate $x \rightarrow x/L$ and we assume quasi-one-dimensional geometry. At the interface, we have two boundary conditions:

$$J_\omega = 2 \sum_{\lambda=1,2} (\delta_\lambda/\gamma_\lambda) \sin \theta_B \sin \theta_{s\lambda} \sin \psi, \quad (2a)$$

$$\partial_x \theta_B = 2 \sum_{\lambda=1,2} \frac{\cos \theta_{s\lambda} \sin \theta_B}{\gamma_\lambda} [\delta_\lambda \tan \theta_{s\lambda} \cot \theta_B \cos \psi - 1]. \quad (2b)$$

Here, J_ω denotes the first integral of Eq. (1b), index λ labels different bands, $\psi = (\phi - 2\chi_B)/2$ and ϕ stands for the global superconducting phase difference across the junction, while factors $\delta_\lambda = \pm 1$ account for the relative shifts of phases between the bands, and finally parameters γ_λ represent dimensionless interface resistances. We also used notations $\theta_B = \theta(\omega, \pm 1/2)$ and similar for χ_B , and introduced Green's functions of a superconductor in the bulk: $\sin \theta_{s\lambda} = |\Delta_\lambda|/\sqrt{|\Delta_\lambda|^2 + \omega^2}$ and $\cos \theta_{s\lambda} = \omega/\sqrt{|\Delta_\lambda|^2 + \omega^2}$, with Δ_λ being corresponding gaps. Having solved Usadel equations, one can find a density of states

$$N(\varepsilon, x)/N_0 = \text{Re}[\cos(\omega, x)]_{\omega \rightarrow i\varepsilon} \quad (3)$$

upon analytical continuation to real energies, and a Josephson current-phase relationship

$$eI(\phi)R_N = 2\pi T \sum_\omega J_\omega = \int \tanh \frac{\varepsilon}{2T} \text{Im} J_\varepsilon d\varepsilon \quad (4)$$

upon summation over Matsubara frequencies, where N_0 is bare density of states in a metal and $R_N = L/e^2 D N_0 S$ is normal state wire resistance of cross-section area S .

III. DENSITY OF STATES

Consider a symmetric $s|n|s$ junction. In the absence of superconducting phase difference between the leads we have $\chi = 0$ and the whole system of equations simplifies to one:

$$\partial_x^2 \theta - (2\omega/\varepsilon_{Th}) \sin \theta = 0, \quad (5)$$

which has to be solved for $x \in [-1/2, 1/2]$. Since this is the same equation as for the nonlinear pendulum it can be integrated exactly in terms of the Jacobi elliptic functions. Indeed, the above equation has a simple first integral:

$$(\partial_x \theta)^2 = (4\omega/\varepsilon_{Th}) [\cos \theta_0 - \cos \theta], \quad (6)$$

where integration constant $\theta_0 = \theta(\omega, 0)$ was chosen to be at the middle of the wire due to obvious symmetry reasons. To perform a subsequent second integration, we change variables as

$$\cos \theta = \frac{2m \cos^2 \phi}{1 - m \sin^2 \phi} - 1, \quad m = \cos^2(\theta_0/2), \quad (7)$$

and find

$$x \sqrt{\frac{2\omega}{\varepsilon_{Th}}} = \int_0^\phi \frac{d\phi}{\sqrt{1 - m \sin^2 \phi}}, \quad (8)$$

which is a tabulated integral. Finally, using the Jacobi elliptic functions cn and dn , the solution appears in the form

$$\cos[\theta(\omega, x)/2] = \cos(\theta_0/2) \frac{\text{cn}(u, m)}{\text{dn}(u, m)}, \quad u = x \sqrt{\frac{2\omega}{\varepsilon_{Th}}}. \quad (9)$$

It is important to keep in mind that the modulus of the Jacobi functions is actually an energy-dependent function $m(\omega)$, see Eq. (7). By using now Eq. (9) in the boundary condition Eq. (2b), one finds a closed algebraic equation for the unknown integration coefficient in the form

$$u_B \sqrt{1+m} \frac{\text{sn}(u_B, m)}{\text{dn}(u_B, m)} + \mathcal{F} \frac{\text{cn}(u_B, m)}{\text{dn}^2(u_B, m)} = \frac{\mathcal{G}}{\sqrt{m(1-m)}} \left[\frac{1}{2} - \frac{1-m}{\text{dn}^2(u_B, m)} \right] \quad (10)$$

where $u_B = \sqrt{\omega/2\varepsilon_{Th}}$, and

$$\mathcal{G}(\omega) = \sum_\lambda \cos \theta_{s\lambda} / \gamma_\lambda = \sum_\lambda \frac{\omega}{\gamma_\lambda \sqrt{|\Delta_\lambda|^2 + \omega^2}}, \quad (11)$$

$$\mathcal{F}(\omega) = \sum_\lambda \delta_\lambda \sin \theta_{s\lambda} / \gamma_\lambda = \sum_\lambda \frac{\delta_\lambda |\Delta_\lambda|}{\gamma_\lambda \sqrt{|\Delta_\lambda|^2 + \omega^2}}. \quad (12)$$

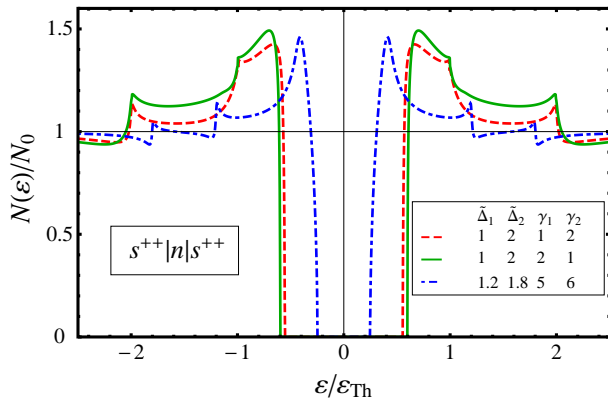


FIG. 1: Representative density of states spectrum in the normal wire as induced by the proximity effect between two s^{++} two-band superconductors. Inset shows parameters, and bulk gaps were normalized to the Thouless energy $\tilde{\Delta}_\lambda = \Delta_\lambda/\varepsilon_{Th}$.

Equation (10) defines m and thus θ_0 as a function of energy ω and together with Eqs. (3) and (9) it provides a complete analytical solution for the Green's function in the wire.

In particular, we can find density of states in the middle of the wire as $N(\varepsilon)/N_0 = \text{Re}[2m(i\varepsilon) - 1]$, which exhibits very rich structure. Indeed, Fig. 1 shows representative profiles of $N(\varepsilon)$ in $s^{++}|n|s^{++}$ junction for different choice of parameters. One finds a proximity-induced energy gap ε_g in the spectrum of a wire, which scales with the Thouless energy $\varepsilon_g \sim \varepsilon_{Th}$. Asymptotic analysis near the gap, $\varepsilon - \varepsilon_g \ll \varepsilon_g$, shows that DOS has a square-root singularity $N(\varepsilon) \propto \sqrt{\varepsilon/\varepsilon_g - 1}$, similar to that in a single-band $s|n|s$ junctions.³⁶ $N(\varepsilon)$ then rapidly grows, passes through the maximum and has two additional peak-like features at higher energies near the superconductive band gaps Δ_λ . This picture has to be contrasted to the DOS profile in $s^{+-}|n|s^{+-}$ junctions shown in Fig. 2. The low-energy behavior is similar but the energy gap is reduced due to anti-proximity effect induced by the π -shifted band. The conceptual difference appears near the band gaps Δ_λ where instead of peaks one finds Fano-like antisymmetric features. This important detail is specific for the s^{+-} symmetry case and can be looked for in the tunneling experiments.

IV. JOSEPHSON CURRENT

Phase-sensitive measurements are clearly more challenging. Nevertheless, we develop a theory for the Josephson effect in mesoscopic $s|n|s^{+-}$ circuits with the idea that some limits considered here will be useful for the future experiments.

In the presence of a superconducting phase gradient in the wire finding an analytical solution of Usadel equations represents a difficult technical problem. In the limit of the long junctions however $L \gg \sqrt{D/T}$ calculation of the Josephson current simplifies considerably. In this

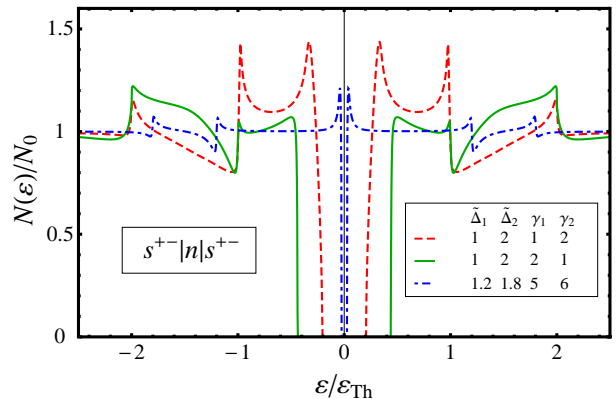


FIG. 2: Representative density of states spectrum in the normal wire as induced by the proximity effect between two s^{+-} two-band superconductors. The anti-symmetric Fano-like features near the gap edges $\tilde{\Delta}_\lambda = \Delta_\lambda/\varepsilon_{Th}$ may provide a definite fingerprint of s^{+-} -superconductivity.

case, it is possible to neglect the mutual role of superconducting leads and introduce an ansatz for the anomalous Green's function $F = e^{i\phi/2} \sin \theta^R + e^{-i\phi/2} \sin \theta^L$, where the functions $\theta^{R(L)}$ satisfy the same sin-Gordon equation as in the case of DOS calculations. Solving it separately near right (left) boundary for $\theta^{R(L)}$ respectively we find³⁷

$$\tan[\theta^{R(L)}(x, \omega)/4] = \mathcal{B}_{R(L)}(\omega) \exp[\pm(x \mp 1/2)L/\xi_\omega] \quad (13)$$

where we introduced coherence length $\xi_\omega = \sqrt{D/2\omega}$. This approximation conserves the current in the normal layer with the exception of the narrow region of the order $\xi_{\omega=T}$ near the boundaries. The two integration coefficients $\mathcal{B}_{R(L)}$ are to be found from the boundary conditions Eq. (2b) at both interfaces, which can be reduced to the algebraic equation:

$$4\mathcal{G}_\alpha(\mathcal{B}_\alpha - \mathcal{B}_\alpha^3) - \mathcal{F}_\alpha(1 - 6\mathcal{B}_\alpha^2 + \mathcal{B}_\alpha^4) = \pm 2(L/\xi_\omega)(\mathcal{B}_\alpha + \mathcal{B}_\alpha^3), \quad \alpha = R, L \quad (14)$$

where \mathcal{G} and \mathcal{F} -functions were defined earlier in Eqs. (11) and (12). With this at hand, we find Josephson current in the form

$$eI(\phi)R_N = 128\pi T \sin \phi \sum_{\omega>0} \frac{L}{\xi_\omega} \mathcal{B}_R(\omega) \mathcal{B}_L(\omega) e^{-L/\xi_\omega} \quad (15)$$

which is applicable in the broad range of temperatures $\varepsilon_{Th} \ll T \lesssim |\Delta_\lambda|$. At lowest temperatures $T \ll \varepsilon_{Th}$, the current-phase relationship in Eq. (15) deviates from being simply sinusoidal because a separable approximation for F -function fails to account properly for the proximity-induced Thouless gap. Unfortunately, analytical calculation of $I(\phi)$ is not possible in this limit, however one may easily estimate the magnitude of the critical current as $eI_c R_N \sim \varepsilon_{Th}$. Furthermore, it is expected that $I(\phi)$ will be nonanalytical function near $\phi = \pi$ since the proximity gap closes at that point while the current is proportional to its derivative $I(\phi) \propto \partial_\phi \varepsilon_g(\phi)$.

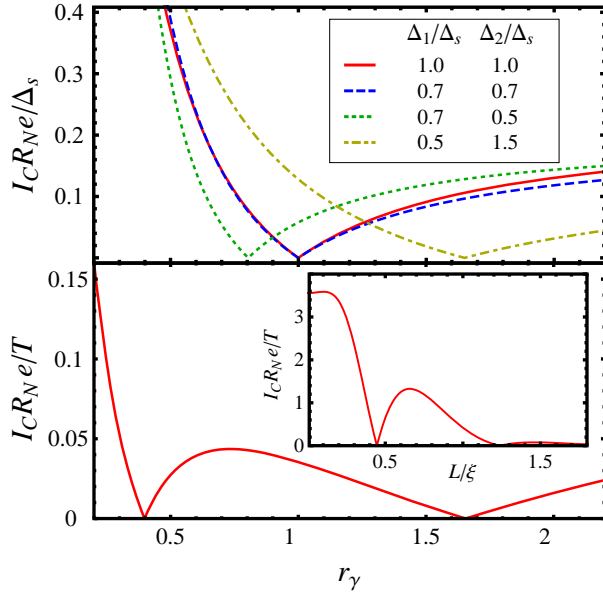


FIG. 3: (Top) Critical current for $s|n|s^{+-}$ junction vs boundary resistance mismatch r_γ . In the inset, Δ_s labels the gap of an ordinary superconductor, while $\Delta_{1,2}$ are the two gaps of an s^{+-} superconductor. The other parameters are $T = 0.5\Delta_s$, $\gamma_1 = \gamma_s = 5$, and $L/\xi_{\pi T} = 2$. (Bottom) Critical current for $s|f|s^{+-}$ junction vs boundary resistance mismatch r_γ for $T = 0.3\Delta_s$, $\Delta_1 = 0.5\Delta_s$, $\Delta_2 = 1.5\Delta_s$, and $h = 3\Delta_s$.

We plot in Fig. 3 the critical current from Eq. (15) as a function of the ratio between the interface barriers for each band $r_\gamma = \gamma_1/\gamma_2$. It is well known that for the conventional superconductors, I_c decays monotonously with r_γ , however, for $s|n|s^{+-}$ junction critical current displays clear $0 - \pi$ switching.^{23,25,28,31} This effect is magnified in the presence of ferromagnetic layer. Including the exchange field h in Eq. (1a) as $\omega \rightarrow \omega + ih \text{sign}(\omega)$, but ignoring spin-flip and spin-orbital scattering, we find from the linearized Usadel equations the current in $s|f|s^{+-}$ junction $I(\phi) = I_c \sin \phi$ with

$$eI_c R_N = 4\pi T \sum_{\omega=-\infty}^{\infty} \frac{(L/\xi_{|\omega|})(\mathcal{F}_R \mathcal{F}_L / \mathcal{G}_R \mathcal{G}_L) / \cosh(L/\xi_{|\omega|})}{(1 + \Gamma_\omega^2) \tanh(L/\xi_{|\omega|}) + \Gamma_\omega \mu_\omega} \quad (16)$$

where $\Gamma_\omega = L/2\xi_{|\omega|} \sqrt{\mathcal{G}_R \mathcal{G}_L}$ and $\mu_\omega = (\mathcal{G}_R + \mathcal{G}_L) / \sqrt{\mathcal{G}_R \mathcal{G}_L}$. Equation (16) is the generalization of the Buzdin formula³⁸ for the multi-band case. Lower panel of Fig. 3 shows enhanced $0 - \pi$ oscillations of the critical current as a function of r_γ , which displays two zero points. Such a peculiar feature is due to the combination of a ferromagnet and s^{+-} superconductor.

In the Josephson junction with extremely low barrier transparency when $\gamma_\lambda \gg 1$, one can circumvent the need of solving Usadel equation in the wire since current is largely determined by the interface. Superconductive phase ϕ changes discontinuously at the barriers and stays nearly zero within the interior of the wire while Green's function phase θ is approximately constant. Since $J_\omega \propto \gamma^{-1} \ll 1$, then to the leading order, one can

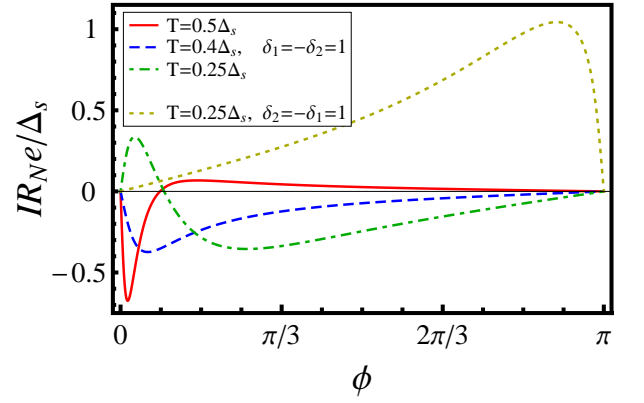


FIG. 4: Josephson current-phase relationship for short $s|n|s^{+-}$ junction for gaps $\Delta_1 = 0.5\Delta_s$, $\Delta_2 = 1.5\Delta_s$, and interface parameters $\gamma_s = 2$, $\gamma_1 = 2.4$, $\gamma_2 = 1.8$.

set $\chi_B = 0$ in Eq. (2a) and $\partial_x \theta = 0$ in Eq. (2b). These approximations allow to find the spectral current,

$$J_\omega = \mathcal{F}^2 \sin \phi \left[\mathcal{G}^2 + \mathcal{F}^2 \cos^2 \frac{\phi}{2} \right]^{-1/2}, \quad (17)$$

where we assumed $s^{+-}|n|s^{+-}$ geometry. For the equal gaps case $\Delta_1 = \Delta_2 \equiv \Delta_s$, above the spectral current J_ω leads to the Josephson current-phase relationship from Eq. (4):

$$eI(\phi)R_N = \frac{\mu^2(1+r_\gamma)}{2\gamma_1} \Delta_s \sin \phi \times \int_{\mu\Delta_s \cos \frac{\phi}{2}}^{\Delta_s} \frac{\tanh(\varepsilon/2T) d\varepsilon}{\sqrt{\Delta_s^2 - \varepsilon^2} \sqrt{\varepsilon^2 - \mu^2 \Delta_s^2 \cos^2 \frac{\phi}{2}}} \quad (18)$$

where $r_\gamma = \gamma_1/\gamma_2$ and $\mu = (1-r_\gamma)/(1+r_\gamma)$. Interestingly, in the zero-temperature limit, even the remaining energy integral can be completed in the closed form, such that we find a Josephson current

$$eI(\phi)R_N = \frac{(\gamma_2 - \gamma_1)^2 \Delta_s \sin \phi}{\gamma_1 \gamma_2 (\gamma_1 + \gamma_2)} K \left[1 - \left(\frac{\gamma_2 - \gamma_1}{\gamma_2 + \gamma_1} \right)^2 \cos^2 \frac{\phi}{2} \right], \quad (19)$$

where $K(x)$ is the complete elliptic integral of the first kind. In the completely symmetric case (with equal transparencies for both bands), the Josephson current vanishes, since the π -shifted bands drive it in the opposite directions. However, including interband scattering effects may result in additional nonvanishing contributions.²⁷

Analytical results are also possible for arbitrary transparencies but for the short junctions when $L \ll \xi_{\omega=\Delta_s}$. In this case, Usadel equations are dominated by the gradient terms. Despite the fact that they remain coupled and nonlinear, all integrations can be completed in the closed form.³⁹ By using the first integral of Eq. (1b), $J_\omega = \sin^2 \theta \partial_x \chi$ and excluding $\partial_x \chi$ from Eq. (1a), one

finds

$$\partial_x^2 \theta = \frac{J_\omega^2 \sin(2\theta)}{2 \sin^4 \theta}. \quad (20)$$

This nonlinear differential equation is solved by

$$\cos[\theta(x, \omega)] = \cos \theta_0 \cos[J_\omega(x - x_0)/\sin \theta_0]. \quad (21)$$

Knowing $\theta(x, \omega)$, one can now calculate the second integral of Eq. (1b),

$$\chi - \chi_0 = J_\omega \int_{x_0}^x \frac{dx}{\sin^2 \theta}, \quad (22)$$

which reads

$$\sin \theta_0 \tan[\chi(x, \omega) - \chi_0] = \tan[J_\omega(x - x_0)/\sin \theta_0]. \quad (23)$$

Having found explicit solutions for the Green's functions, the boundary problem for the integration coefficients can be reduced to solving three algebraic equations:

$$J_\omega = \mathcal{F}_L \sin \theta_B \sin(\chi_B + \phi/2), \quad (24)$$

$$J_\omega = \mathcal{F}_R \sin \theta_B \sin(\phi/2 - \chi_B), \quad (25)$$

$$\begin{aligned} & \mathcal{F}_L \cos \theta_B \cos(\chi_B + \phi/2) - \mathcal{G}_L \sin \theta_B \\ &= \mathcal{F}_R \cos \theta_B \cos(\chi_B - \phi/2) - \mathcal{G}_R \sin \theta_B. \end{aligned} \quad (26)$$

These expressions finally lead us to the Josephson current-phase relationship in the form

$$eI(\phi)R_N = 8\pi T \sum_{\omega} \frac{\mathcal{A}(\phi) \sin \phi}{\mathcal{F}_R^{-1} + \mathcal{F}_L^{-1}} \left[\mathcal{A}^2(\phi) + \frac{(\mathcal{G}_R - \mathcal{G}_L)^2}{(\mathcal{F}_R - \mathcal{F}_L)^2} \right]^{-\frac{1}{2}}, \quad (27)$$

where

$$\mathcal{A}(\phi) = \left[\cos^2 \frac{\phi}{2} + \frac{(\mathcal{F}_R - \mathcal{F}_L)^2}{(\mathcal{F}_R + \mathcal{F}_L)^2} \sin^2 \frac{\phi}{2} \right]^{-1/2}. \quad (28)$$

A representative feature of Eq. (27) is that $I(\phi)$ switches its sign in between $\phi = 0$ and $\phi = \pi$ as shown in Fig. 4. This implies that the free energy of $s|n|s^{+-}$ junction has two minima and such junction may be used as the phase inverted in superconducting digital circuits. Such feature, however, is not unique for s^{+-} superconductors and can be realized in other complex hybrid circuits with ordinary materials.⁴⁰

In summary, we have studied the density of states and Josephson current in mesoscopic circuits with unconventional s^{+-} superconductors. We find that tunneling spectra have distinct fingerprints of the sign changing symmetry of the underlying superconductive order parameter induced by the proximity effect. Furthermore, the critical current exhibits a robust π junction even in the absence of the ferromagnetic layer. The Josephson current-phase relationship itself is not indicative of s^{+-} symmetry due to the sensitivity to parameters defining the junction.

We would like to thank Maxim Vavilov for useful discussions, Valentin Stanev for correspondence regarding Ref. 29, and Norman Birge for reading and commenting on the paper. This work was supported by Michigan State University.

-
- ¹ I. I. Mazin and J. Schmalian, *Physica C* **469**, 614 (2009).
² J. Paglione and R. L. Greene, *Nat. Phys.* **6**, 645 (2010).
³ A. Chubukov, *Ann. Rev. Cond. Mat. Phys.* **3**, 57 (2012).
⁴ H. Luetkens, H.-H. Klauss, M. Kraken, F. J. Litterst, T. Dellmann, R. Klingeler, C. Hess, R. Khasanov, A. Amato, C. Baines, M. Kosmala, O. J. Schumann, M. Braden, J. Hamann-Borrero, N. Leps, A. Kondrat, G. Behr, J. Werner, and B. Büchner, *Nature Mater.* **8**, 305 (2009).
⁵ A. J. Drew, Ch. Niedermayer, P. J. Baker, F. L. Pratt, S. J. Blundell, T. Lancaster, R. H. Liu, G. Wu, X. H. Chen, I. Watanabe, V. K. Malik, A. Dubroka, M. Rössle, K. W. Kim, C. Baines, and C. Bernhard, *Nature Mater.* **8**, 310 (2009).
⁶ A. V. Chubukov, D. V. Efremov, and I. Eremin, *Phys. Rev. B* **78**, 134512 (2008).
⁷ A. B. Vorontsov, M. G. Vavilov, and A. V. Chubukov, *Phys. Rev. B* **81**, 174538 (2010).
⁸ R. M. Fernandes and J. Schmalian, *Phys. Rev. B* **82**, 014521 (2010).
⁹ I. I. Mazin, D. J. Singh, M. D. Johannes, and M. H. Du, *Phys. Rev. Lett.* **101**, 057003 (2008).
¹⁰ K. Kuroki, S. Onari, R. Arita, H. Usui, Y. Tanaka, H. Kon-tani, and H. Aoki, *Phys. Rev. Lett.* **101**, 087004 (2008).
¹¹ V. Barzykin and L. P. Gorkov, *JETP Lett.* **88**, 131 (2008).
¹² K. Seo, B. A. Bernevig, and J. Hu, *Phys. Rev. Lett.* **101**, 206404 (2008).
¹³ T. A. Maier, S. Graser, D. J. Scalapino, P. J. Hirschfeld,, *Phys. Rev. B* **79**, 224510 (2009).
¹⁴ A. V. Chubukov, M. G. Vavilov, and A. B. Vorontsov, *Phys. Rev. B* **80**, 140515(R) (2009).
¹⁵ A. D. Christianson, E. A. Goremychkin, R. Osborn, S. Rosenkranz, M. D. Lumsden, C. D. Malliakas, I. S. Todorov, H. Claus, D. Y. Chung, M. G. Kanatzidis, R. I. Bewley, T. Guidi, *Nature* **456**, 930 (2008).
¹⁶ X. Zhang, Y. S. Oh, Y. Liu, L. Yan, K. H. Kim, R. L. Greene, and I. Takeuchi, *Phys. Rev. Lett.* **102**, 147002 (2009).
¹⁷ Y.-R. Zhou, Y.-R. Li, J.-W. Zuo, R.-Y. Liu, S.-K. Su, G. F. Chen, J. L. Lu, N. L. Wang, Y.-P. Wang, arXiv:0812.3295.
¹⁸ T. Hanaguri, S. Niitaka, K. Kuroki, H. Takagi, *Science* **328**, 474 (2010).
¹⁹ C.-T. Chen, C. C. Tsuei, M. B. Ketchen, Z.-A. Ren, and Z. X. Zhao, *Nat. Phys.* **6**, 260 (2010).

- ²⁰ D. Parker and I. I. Mazin, Phys. Rev. Lett. **102**, 227007 (2009); A. A. Golubov and I. I. Mazin, arXiv:1209.2944.
- ²¹ J. Wu and P. Phillips, Phys. Rev. B **79**, 092502 (2009).
- ²² T. K. Ng and N. Nagaosa, Europhys. Lett. **87**, 17003 (2009).
- ²³ J. Linder, I. B. Sperstad, and A. Sudbo, Phys. Rev. B **80**, 020503(R) (2009).
- ²⁴ W.-F. Tsai, D.-X. Yao, B. A. Bernevig, and J. P. Hu, Phys. Rev. B **80**, 012511 (2009).
- ²⁵ W.-Q. Chen, F. Ma, Z.-Y. Lu, and F.-C. Zhang, Phys. Rev. Lett. **103**, 207001 (2009).
- ²⁶ Y. Ota, M. Machida, T. Koyama, and H. Matsumoto, Phys. Rev. Lett. **102**, 237003 (2009); *ibid* Phys. Rev. B **81**, 214511 (2010).
- ²⁷ Yu. Erin and A. N. Omelyanchuk, Low. Temp. Phys. **36**, 969 (2010).
- ²⁸ E. Berg, N. H. Lindner and T. Pereg-Barnea, Phys. Rev. Lett. **106**, 147003 (2011).
- ²⁹ A. E. Koshelev and V. Stanev, Europhys. Lett. **96**, 27014 (2011); *ibid* Phys. Rev. B **86**, 174515 (2012); A. E. Koshelev, arXiv:1209.5438.
- ³⁰ S.-Z. Lin, Phys. Rev. B **86**, 014510 (2012).
- ³¹ V. Vakaryuk, V. Stanev, W.-C. Lee, A. Levchenko, Phys. Rev. Lett. **109**, 227003 (2012).
- ³² K. D. Usadel, Phys. Rev. Lett. **25**, 507 (1970).
- ³³ M. Kupriyanov and V. F. Lukichev, Sov. Phys. JETP **67**, 1163 (1988).
- ³⁴ A. Brinkman, A. A. Golubov, and M. Y. Kupriyanov, Phys. Rev. B **69**, 214407 (2004).
- ³⁵ W. Belzig, F. K. Wilhelm, C. Bruder, G. Schön, A. D. Zaikin, Superlat. and Microstruct. **25**, 1251 (1999).
- ³⁶ A. Levchenko, Phys. Rev. B **77**, 180503 (2008).
- ³⁷ A. D. Zaikin and G. F. Zharkov, Sov. J. Low. Temp. Phys. **7(3)**, 184 (1981).
- ³⁸ A. Buzdin and I. Baladié, Phys. Rev. B **67**, 184519 (2003).
- ³⁹ A. Levchenko, A. Kamenev and L. Glazman, Phys. Rev. B **74**, 212509 (2006).
- ⁴⁰ A. A. Golubov, M. Yu. Kupriyanov and E. Il'ichev, Rev. Mod. Phys. **76**, 411 (2004).